RFIDrone: Preliminary Experiments and Electromagnetic Models

M. Longhi, G. Casati, D. Latini, F. Carbone, F. Del Frate and G. Marrocco

*Department of Civil Engineering and Computer Science, University of Rome Tor Vergata, Italy
e-mails: michela.longhi@uniroma2.it, guido.casati@uniroma2.it, latini@disp.uniroma2.it, carbonefrancesco84@gmail.com
delfrate@disp.uniroma2.it, gaetano.marrocco@uniroma2.it

***Abstract*—We introduce in a unitary way the paradigm of radiofrequency identification (RFID) merged with the technology of Unmanned Aerial Vehicles (UAV) giving rise to RFIDrone devices. Such family comprises the READER-Drone, which is a suitable UAV integrated with an autonomous RFID reader to act as mobile scanner of the environment, and the TAG-Drone, a UAV only equipped with an RFID sensor tag that hence becomes a mobile and automatically re-positioned sensor. We shows some handy electromagnetic models to identify the upper-bound communication performance of RFIDrone in close proximity of a scattering surface and we resume the results of some preliminary open-air experimentation corroborating the theoretical analysis.**

I. Introduction

RFID technology is now currently orienting from logistic-only applications toward more higher-value sensing systems, hence becoming one of the enabling technologies of the Internet of Things.

Unmanned Aerial Vehicles (UAV) are experiencing a huge growth in both amateur and professional contexts comprising a wide variety of typologies, size and complexities, ranging from micro-drones with very limited autonomy up to small airframe with long-range scope. RFID and UAV technologies are now mature to be merged together thus enabling a set of completely new application fields. A few researchers and companies have already envisaged this potentials and some very preliminary experimentations may be found over conventional scientific channels. It is conceived that an UAV could be equipped with an RFID scanner in the UHF band [1] and this moving agent could collect identification and sensing information from RFID tags displaced in harsh environments [2] like bridges [3], trees, open air warehouses [4], [5]. Accordingly, the preliminary envisaged applications are Structural Health Monitoring [6], Precise Agriculture, Automated Inventory in large areas [7], Animal Surveillance [8] and Environmental Monitoring [9], [10]. The RFID-UAV research field, hereafter referred to as *RFIDrone* is however still in its infancy and most of the relevant topics and some configurations and options have to be investigated and systematized.

This contribution introduces the electromagnetic aspects of two possible architectures of RFIDrone systems that differs for the specific integration of the UAV with either the reader or the tag devices. We show some preliminary electromagnetic models allowing to understand the upper bounds of the expected identification performance. We also summarize some real-life measurements with a professional airframe interacting with several RFID sensors in an open field.

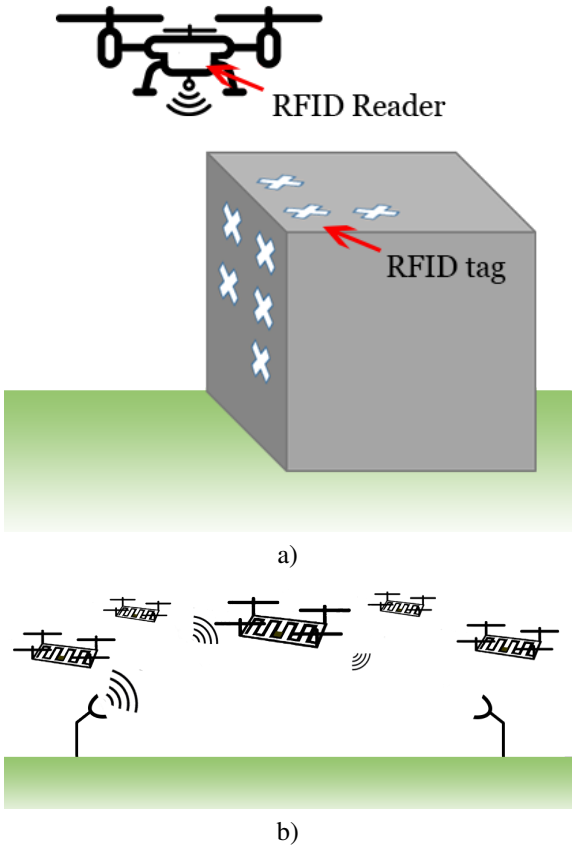

Figure 1. Topologies of RFIDrones: a) Reader-Drone hosting an RFID reader and interacting with fixed sensors displaced over an infrastructure; b) Tag-Drone where a sensor-RFID tag is equipped with flight capability and interacts with a fixed base station for data exchange and assisted localization.

II. RFIDrone Topologies and Possible Applications

The RFIDrone concept can be discussed in more generality by considering the two complementary paradigms of

READER-Drone (herafter R-drone) and *TAG-Drone* (hereafter T-drone).

A. R-drone

A suitable UAV is integrated with an autonomous RFID reader to act as mobile scanner of the environment (Fig.1a). The drone can be remotely driven to approach tags displaced onto a surface ad equipped with sensors. Alternatively, the R-drone may be programmed to autonomously and periodically approach sensors and retrieve sensed data. Sampled data may be stored onboard for a late-time recovery when the drone comes back or may be instead transmitted in real time to a fixed base-station placed in radio visibility with the drone itsef.

The electromagnetic issues of this configuration are the achievable maximum read range and the footprint of the reader onto the surface of the soil/infrastructure hosting the displaced sensors.

B. T-drone

The UAV is only equipped with an RFID sensor tag that hence becomes a mobile and automatically re-positioned sensor. From a different perspective, this object can be interpreted as a sensor with flying capability in order to highlight that only elementary UAV features are expected (Fig.1b). The T-drone may be used in standalone mode or according to the more fascinating swarm configuration (like bees) cooperatively collecting information within a same environment. T-drones should have small size so that they could be referred to the technology of micro-drones.

R-drones and T-drones may mutually interact like a conventional RFID network but in this case the R-drone could act as a *mother* drone moving and mastering a swarm of T-drones.

Promising applications are the volumetric scanning of environments. A swarm of T-drones with environmental-oriented sensor capabilities (temperature, humidity, pressure, specific gases) will methodically fly within a large volume (inside stations, airports, factories, large green-house) at the purpose to provide a 3D map of those parameters. Application to the air quality enforcement and to the optimization of heat generation and thermal distribution systems. The T-drone could include a data-logger capability and in this case the stored information could be downloaded by an external system when the T-drone comes back home or when it gets closer to a network of readers (gates).

Electromagnetic issues are hence the design of drone-oriented RFID tags and the localization of the micro-drone, for instance by using a network of fixed interrogating antennas in the close surrounding of the micro-drone that will process the field backscattered by the micro-drone itself.

III. Parametric Electromagnetic Modeling

Unlike conventional applications of UAV, an RFIDrone system in the reader mode has to fly at a close distance to sensorized surfaces and hence the read region of the reader, as well as the portion of that surface that is instantaneously

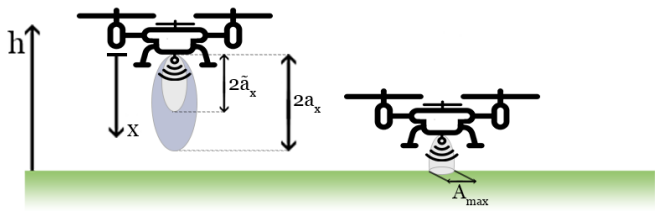

Figure 2. A schematic ellipsoidal representation of the reading zone of an R-drone evaluated with the free space hypothesis (dark gray, major axis a_x) and including the effect of the infrastructure in front of the drone (light gray, major axis $\tilde{a_x}$).

visible to the drone (footprint), is related to several parameters such as

- $EIRP$ of the reader (thus including the maximum radiated power allowed to the portable reader installed onboard and the antenna gain)
- *h*: the distance between the drone and the surface
- BWx BWy: the beamwidth of the reader's antenna on the principal cuts
- $\tilde{G}_T$: the realized gain of the tag sensor
- P_C: the sensitivity of the tag microchip.
- Γ: the amplitude of the Fresnel reflection coefficient of the surface hosting the tag.

In the free-space, the read region of a reader placed at position $x = 0$ and radiating toward $x > 0$, e.g. the space where a tag with effective microchip sensitivity

$$\tilde{p}_C = \frac{P_C}{\tilde{G}_T} \tag{1}$$

collects enough power to be energized and send back its ID, can be roughly approximated by an ellipsoid (Fig.2) whose axis a_ξ (with $\xi = \{x, y, z\}$) are related [11] to the electrical parameter of the link, e.g.

$$a_x = \frac{\lambda}{8\pi}\sqrt{\chi\frac{EIRP}{\tilde{p}_C}} \tag{2}$$

$$a_\xi = a_x\sqrt{tan\frac{BW_{x_\xi}}{2}\frac{sin\frac{BW_{x_\xi}}{2}}{\sqrt{2}-cos\frac{BW_{x_\xi}}{2}}} \tag{3}$$

The maximum read distance corresponds therefore to twice the major axis $r_{FS} = 2a_x$.

For the RFIDrone scenario (Fig. 2) instead, the presence of a strongly reflecting infrastructure at a close distance to the reader forbids the use of the free-space equations. That read distance can be nevertheless corrected by a simple two-ray propagation model accounting for the distance and the reflection coefficient of the surface. Hence, the more realistic ellipsoidal representation of the reading distance is such that the corrected major axis $\tilde{a}_x$ is a solution of the polynomial equation which is obtained from the combination of the reading volume and the field projector equations under the condition of reflection by an obstacle:

$$\tilde{a}_x^2 - \left[\frac{h}{2} + (1+\Gamma)a_x\right]\tilde{a}_x + h \cdot a_x = 0 \tag{4}$$

that, for the particular case of a perfectly conducting wall simply becomes

$$\tilde{a}_x = \frac{h}{2} + a_x - \frac{1}{2}\sqrt{h^2 + 4a_x^2} \tag{5}$$

The footprint of the R-drone over the surface is hence an ellipse given by the intersection of the above ellipsoid with the plane $x = h$. The diameter of the footprint is given by:

$$A_{max} = 2\,a_{max}\sqrt{\frac{1}{2}\left[1 - \frac{(h-\tilde{a}_x)^2}{\tilde{a}_x^2}\right]} \tag{6}$$

where $a_{max} = max\{a_y,\, a_z\}$.

Fig.3 shows the major axis of the reader footprint, versus the distance h, corresponding to some realistic values of the reader's EIRP, the beam-width of the reader's antenna resembling a dipole-like (BW=90°) and a patch-like (BW=60°) configuration, and finally the effective microchip sensitivity $\widetilde{p}_C$ = {-5dBmW, -15dBmW, -30dBmW} resembling, respectively, a battery-less sensing chip, an identification-only chip and a battery-assisted sensing chip. There is an optimal distance between the R-drone and the surface allowing the largest interrogation footprint which can be enlarged by using low-directivity antennas. The sensitivity of the chip is however the most critical parameter and the detection of tags equipped with battery-less sensing chips will be rather challenging since the R-drone should fly at less than 50 cm from the surface for all the considered configurations. Moreover, the size of the footprint is of the order of 10 cm and hence comparable with the size of the sensor itself. Battery-assisted sensor tags will be instead easily detectable within a footprint up to more than 3 m (and more than 1m even in case of low-power readers) when the reader-drone flies up to 5 m and more from the surface.

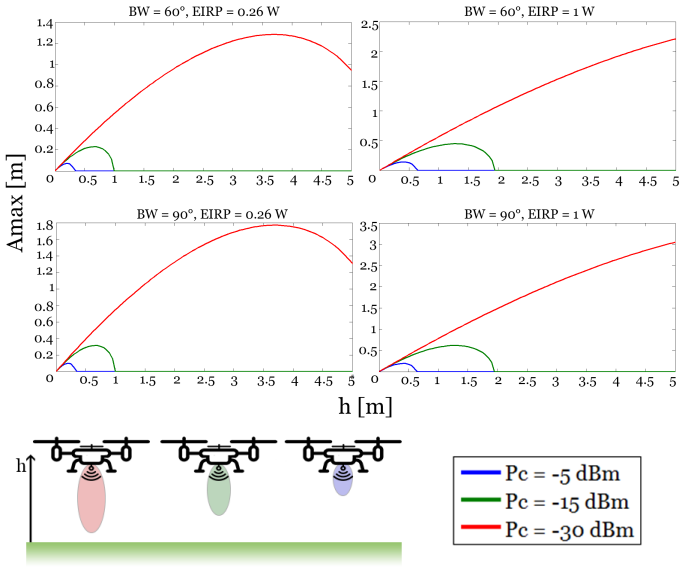

Figure 3. Maximum size of the footprint of the R-drone over a surface (with reference reflection coefficient $\Gamma = 0.5$) hosting the sensors versus the distance h from the drone for several combinations of reader's EIRP and beamwidth and chip sensitivity.

IV. Open-air Experimentation

A first experiments with the R-drone and the T-Drone architectures involved a FlyTop FlyNovex drone (Fig.4a) having 7 kg net weight, 4 kg maximum payload, 20 minutes of autonomy and flying at up to 50 km/h.

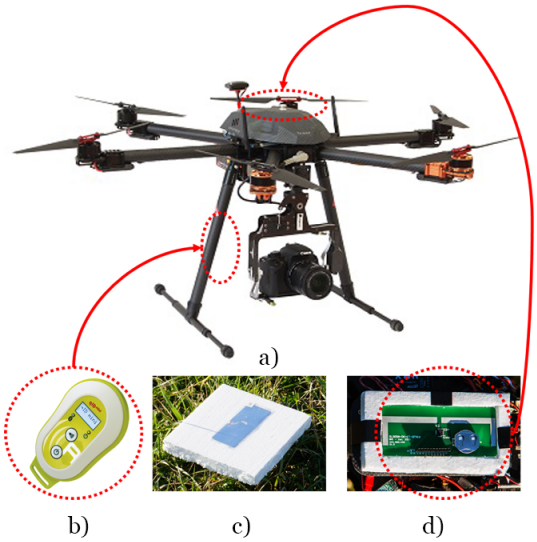

Figure 4. a) Drone FlyTop FlyNovex; b) onboard reader; c) dipole-tag attached over a foam layer and connected to a dielectric post for easy application over the ground, d) RFID data-logger

A. Scanning an array of tags

The R-drone scheme was implemented by installing onboard the portable battery-assisted low-power reader CAEN-RFID qIDmini [12] (Fig.4b) with declared EIRP=0.26 W. The reader was remotely controlled in real time via Bluetooth interface by the RADIO6ENSE RadioSCAN Software [13] running over a notebook. The tags for on-ground deployment were Avery Dennison AD-843 dipoles (Fig.4c) with chip sensitivity Pc=-18 dBmW. Tags were placed over a plain meadows at a 8.5 cm distance from the soil by means of dielectric tubular posts and forming a 6 by 5 array with 0.5 m spacing (Fig.5a). According to the above described link budget, the optimal height of the R-drone over the soil is about 75 cm and the footprint is a circle of diameter 35 cm.

Accordingly, the drone was driven parallel to the array at a fixed distance of about $h = 0.5m$ at a constant velocity of 1m/s in order to scan it by rows. In particular, flying in between two rows, the reader-drone was able to collect the response of two tags at a same time and an example of the received backscattered power signals from the tags of the first two rows is given in Fig.5b.

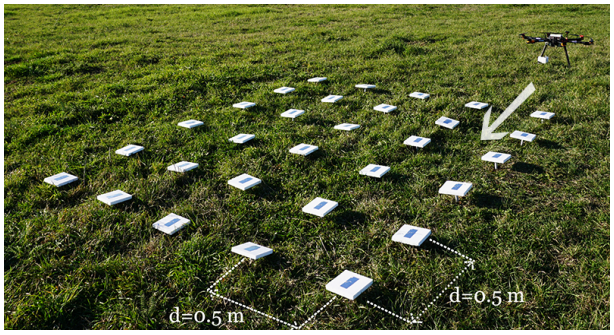

a)

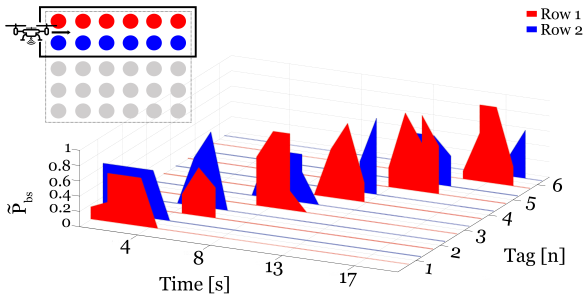

b)

Figure 5. R-drone: a) 5 by 6 array of dipole-like tags over meadow; b) time-variant (normalized backscattered power signals collected when the drone flew in between the first two rows of the array (see inset) and hence capable of interrogating a couplet of adjacent tags at a same time.

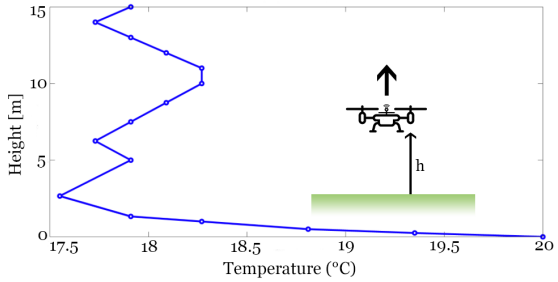

a)

Figure 6. T-drone: Temperature profile measured by the onboard RFID data-logger when the T-drone took-off vertically.

B. Temperature profile measurement by a T-drone

The T-drone modality was implemented by installing aboard the drone (Fig.4d) the semi-active tag SL900A-DK-STQFN16 embedding the SL900A microchip [14], having capability of temperature sensing in the range [-20°C, 165°C] with 0.1°C resolution. The tag is equipped with a 3V battery and can be used as a programmable data-logger suitable to store the sampled data into an internal memory. Once the sensor was activated by a Thing-Magic M6E reader [15], the drone slowly moved vertically from the soil up to a height $h = 15m$ and the temperature was recorded. At the end of the experiment, the collected data were downloaded by the reader and an example of profile is shown in Fig.6.

V. Conclusions

In this work we have presented some electromagnetic bounds and preliminary experimentation of the RFIDrone architecture. The propagation model revealed that using low-sensitivity battery-less tags may yield a great challenge in establishing a robust link between a moving READER-drone and the sensor-tag, especially when the drone has to find the sensor and approach it. Battery-assisted sensor tags, or even solar-cell powered tags, may instead enable a much easier interrogation procedure. The preliminary experimental tests considering the reader-drone configuration have given a first corroboration of the theoretical analysis.

Acknowledgment

Authors wish to thank the two University spin-off GEO-K (www.geo-k.co) and RADIO6ENSE (www.radio6ense.com) for hardware and software support.

References

[1] J. Wang, E. Schluntz,B. Otis, T. Deyle, "A New Vision for Smart Objects and the Internet of Things: Mobile Robots and Long-Range UHF RFID Sensor Tags,", *arXiv preprint whitepaper,* no. 1507.02373, Jul. 2015, available at: http://arxiv.org/pdf/1507.02373.pdf

[2] G. Greco, C. Lucianaz, S. Bertoldo, and M. Allegretti, "A solution for monitoring operations in harsh environment: a RFID reader for small UAV", *In Electromagnetics in Advanced Applications (ICEAA), 2015 International Conference on*, pp. 859-862, Sept. 2015

[3] "Futuristic Inspections for Bridge Safety", *TuftsNow*, Tufts University, May 2014, available at: http://now.tufts.edu/articles/futuristic-inspections-bridge-safety

[4] "The flying inventory assistant", Fraunhofer Institute for Material Flow and Logistics IML, Dec. 2014, available at: https://www.fraunhofer.de/en/press/research-news/2014/december/the-flying-inventory-assistant.html

[5] C. Swedberg, "RFID-Reading Drone Tracks Structural Steel Products in Storage Yard" *RFID Journal*, Sept. 2014, available at: http://www.rfidjournal.com/articles/view?12209/

[6] D. Mascareñas, E. Flynn, M. Todd, G. Park, C. Farrar, "Wireless sensor technologies for monitoring civil structures", *Sound and Vibration,* no. 42, pp. 16-21, Apr. 2008

[7] DeltaDrone - Robotic barcode scanning for large uniform warehouses, www.deltadrone.com

[8] "Kenyan reserve sheltering rare rhinos to launch anti-poaching drone", *Wired Technology*, Jul. 2013, available at: http://www.wired.co.uk/news/archive/2013-07/29/anti-poaching-drone-kenya

[9] G. Greco, C. Lucianaz, S. Bertoldo, and M. Allegretti, "Localization of RFID tags for environmental monitoring using UAV", *In Research and Technologies for Society and Industry Leveraging a better tomorrow (RTSI), IEEE 1st International Forum on*, pp. 480-483, 2015

[10] M. Allegretti, S. Bertoldo, "Recharging RFID Tags for Environmental Monitoring Using UAVs: A Feasibility Analysis," *Wireless Sensor Network*, pp. 13-19, Feb. 2015

[11] G. Marrocco, E. Di Giampaolo, R. Aliberti, "Estimation of UHF RFID Reading Regions in Real Environments," Antennas and Propagation Magazine, IEEE, Vol. 51, pp. 44-57, Dec. 2009

[12] CAENRFID, www.caenrfid.it

[13] Radio6ense, http://www.radio6ense.com

[14] Ams AG, http://ams.com

[15] ThingMagic, http://www.thingmagic.com